Diversity Gain of Lattice Constellation Based Joint Orthogonal Space-Time Block Coding

Wei Liu, Jing Lei, Muhammad-Ali Imran, *Senior Member, IEEE,* and Chaojing Tang

Abstract

It is generally thought that space-time block codes (STBCs) can obtain no more than full space diversity. In this paper, we propose a new construction method of joint orthogonal STBCs based on M dimensional lattice constellations for obtaining space and time diversities simultaneously. By deriving the Chernoff bound of error probability, we prove the exact diversity gain of the proposed code is M times of that in traditional STBCs. This is a valuable scheme as diversity gain is usually the primary factor to determine the ability of anti-fading. Moreover, the maximum-likelihood decoder for the proposed code just requires joint decoding of M real symbols, whose complexity is acceptable as M, usually, needs not to be too big. Numerical results show that the proposed code has remarkable improvement of performance compared with some typical STBCs under the comparable low decoding complexity.

Index Terms

Space-time block code, multiple-input multiple-output, diversity gain, Chernoff bound, multi-dimensional lattice constellation.

I. Introduction

In wireless communications, diversities are very effective strategies to combat the channel fading and improve the reliability, which generally include time-, frequency-, space-, user-, and polarity-diversities, etc., depending on the corresponding multiple physical layer resources provided by the wireless channel and the suitable approaches for exploiting such kind of diversities. In particular, multiple-input multiple-output (MIMO) systems can provide multiple transmission paths along space due to multiple antennas used. As an approach to exploit the space diversity, space-time coding techniques have recently received massive research interest in MIMO systems [1]-[11].

Orthogonal space-time block codes (OSTBC) [1]-[3] offer full space diversity and allow simple single-symbol maximum-likelihood (ML) decoding, but the code rate is always less than one when more than two antennas are used. Later, the rate limitation is overcome by quasi-orthogonal STBCs (QOSTBC) by relaxing the orthogonality and slightly increasing decoding complexity, where rate one is reached for more antennas and full space diversity is

W. Liu, J. Lei and C. Tang are with the College of Electronic Science and Engineering, National University of Defense Technology, Changsha, Hunan, 410073 China. e-mail: wliu_nudt, leijing, cjtang@nudt.edu.cn.

MA. Imran is with the Centre for Communication Systems Research, University of Surrey, Guildford Surrey, GU2 7XH U.K. e-mail: m.imran@surrey.ac.uk.

achieved by special constellation rotation [4]. On the other hand, the full rate alternatives to orthogonal and quasi-orthogonal STBCs namely the Golden codes [5] and Perfect codes [6], [7] are introduced to obtain higher rate and larger coding gain. However, they generally have a prohibitively high decoding complexity as all the symbols need to be decoded jointly. Recently, some high rate (rate>1) and even full rate codes are presented in [8]-[10] to still preserve the low-complexity decodability properties, which are either group-decodable [8], [9] or fast-decodable [10]. Generally, as a premise of those STBCs to pursue high rate, low complexity, or large coding gain, etc., they first guarantee to achieve full space diversity [11], as diversity gain is often the primary factor to determine the performance of coding against channel fading. The maximum achievable space diversity gain of a space-time code is usually the product $N_T N_R$, where N_T and N_R represent the number of transmit antennas and receive antennas, respectively. Actually, besides multiple space paths in MIMO channel, each of these space paths exhibits numerous degrees of freedom for fading along time, which provide the possibility to exploit time diversity as well. Later, a joint double-Alamouti coding is introduced in [12] to simultaneously achieve space and time diversities and still reserve low complexity of ML decoding. However, [12] just considers the code construction jointing double blocks for the case of $N_T = 2$, and gives a rough analysis of diversity orders. First, it is shown by non-strict physical interpretation from the channel fading that diversity orders is perhaps 4 when $N_R = 1$; then, it is regarded as that the diversity orders is more than 4 by comparing the slope of BER-SNR curve of the new code with other codes when $N_R = 2$. The exact orders of diversity gain cannot be got by such a way of slope comparison. The lack of theoretical analysis and proof for diversity gain is a main shortage of [12].

In this paper, we propose a generic construction method for Lattice-based Joint OSTBCs (LJ-OSTBC), where M blocks are orthogonal-space-time coded jointly based on multi-dimensional lattice constellations [13], [14], [15], and the code in [12] can be regarded as a special case of $M = 2 = N_T$. The main contributions of this work compared with [12] are the following three aspects:

i) As a key and necessary step to construct the LJ-OSTBC, an unified equivalent decoupled model for OSTBCs is derived, where the MIMO channel is converted into many equivalent SISO channels so that multiple blocks can be coded combining lattice constellations to obtain time diversity. In addition, such an decoupled model is also a base for the proposed code reserving low decoding complexity and having practical significance.

ii) We theoretically prove the exact orders of diversity gain by deriving the Chernoff bound of error probability for the constructed codes. The results show that the proposed LJ-OSTBC can obtain MN_TN_R orders diversity gain, which is much bigger than that of traditional STBCs. The result is beyond general concept of space-time coding and also reflects the value of proposed codes.

iii) We present a typical mobile channel of 1.9 GHz personal communications services (PCS) systems in our simulations for evaluating the performance and decoding delay of the proposed code. In such a scenario, these factors of mobility speed, Doppler spread, time-varying and temporal correlation are considered comprehensively. That is a more practical evaluation than that in [12].

The rest of this paper is organized as follows. In Section II, we derive an equivalent decoupled model for OSTBC systems. Then, the construction of LJ-OSTBCs is proposed in Section III. Next, the proof of diversity gain is given in Section IV. The numerical results are provided in Section V. Finally, we draw the conclusions in Section VI.

Notations: where $\mathcal{E}(\cdot)$ denotes the expectation of a random variable; $\mathcal{CN}(m,\sigma^2)$ and $\mathcal{N}(m,\sigma^2)$ represents complex- and real-, respectively, Gaussian distribution with mean m and variance σ^2; $(\cdot)_I$ and $(\cdot)_Q$ denote the real part and imaginary part, respectively, of a vector or matrix; $(\cdot)^T$ stands for the transpose of a vector or matrix; $\|\cdot\|_F$ is the Frobenius norm of a matrix; $\mathbf{I}(\cdot)$ represents a unit matrix; $diag(\cdot)$ denotes diagonalization of a vector to compose a diagonal matrix; $|\cdot|$ represents the absolute value of a complex number.

II. Equivalent Decoupled Model of OSTBC

Let's start from analyzing the property of channel from an OSTBC. Generally, a STBC can be defined by the following linear form of dispersion matrices, as

$$\mathbf{C} = \sum_{k=1}^{K} \mathbf{A}_k x_k \tag{1}$$

where $x_1, x_2, ..., x_K$ are K real signals in the codeword; $\mathbf{A}_1 \sim \mathbf{A}_K$ denote the corresponding complex dispersion matrices with $L \times N_T$ dimensions; and L is the time length of codeword. The code $\mathbf{C}$ also obey the average energy constraint as $\mathcal{E}\|\mathbf{C}\|_F^2 = N_T L$. The corresponding $L \times N_R$ receive matrices is

$$\mathbf{R} = \sqrt{\frac{\rho}{N_T}}\mathbf{C}\mathbf{H} + \mathbf{N} \tag{2}$$

where the factor $\sqrt{\rho/N_T}$ ensures that ρ is the SNR at each receive antenna, and independent on N_T; $\mathbf{H}$ and $\mathbf{N}$ denote the $N_T \times N_R$ channel matrix and $L \times N_R$ noise matrix, respectively; the entries of both $\mathbf{H}$ and $\mathbf{N}$ satisfy i.i.d. complex Gaussian random variables with distribution $\mathcal{CN}(0,1)$. The channel fadings at different antennas are flat and mutually independent. Like common STBCs, we assume that the channel satisfy the block fading, i.e., the channel matrix remains constant within one code block and changes independently during different blocks [11].

Define $\mathbf{r}_j$, $\mathbf{h}_j$ and $\mathbf{n}_j$ as the jth column of $\mathbf{R}$, $\mathbf{H}$, and $\mathbf{N}$, respectively. With some simple mathematical manipulations, we can derive a real vectorized model by combining (1) and (2), as

$$\mathbf{r}' = \sqrt{\frac{\rho}{N_T}}\mathbf{H}'\mathbf{x}_{eq} + \mathbf{n}', \tag{3}$$

where $\mathbf{r}' = [(\mathbf{r}_1)_I^T \quad (\mathbf{r}_1)_Q^T \quad ... \quad (\mathbf{r}_{N_R})_I^T \quad (\mathbf{r}_{N_R})_Q^T]^T$ is a $2LN_R \times 1$ received column vector; $\mathbf{n}' = [(\mathbf{n}_1)_I^T \quad (\mathbf{n}_1)_Q^T \quad ... \quad (\mathbf{n}_{N_R})_I^T \quad (\mathbf{n}_{N_R})_Q^T]^T$ is a $2LN_R \times 1$ noise vector; $\mathbf{x}_{eq} = [x_1 \quad x_2 \quad ... \quad x_K]^T$ is a $K \times 1$ real signal vector; and

$$\mathbf{H}' = \begin{bmatrix} \bar{\mathbf{A}}_1\bar{\mathbf{h}}_1 & \bar{\mathbf{A}}_2\bar{\mathbf{h}}_1 & ... & \bar{\mathbf{A}}_K\bar{\mathbf{h}}_1 \\ \bar{\mathbf{A}}_1\bar{\mathbf{h}}_2 & \bar{\mathbf{A}}_2\bar{\mathbf{h}}_2 & ... & \bar{\mathbf{A}}_K\bar{\mathbf{h}}_2 \\ \vdots & \vdots & \ddots & \vdots \\ \bar{\mathbf{A}}_1\bar{\mathbf{h}}_{N_R} & \bar{\mathbf{A}}_2\bar{\mathbf{h}}_{N_R} & ... & \bar{\mathbf{A}}_K\bar{\mathbf{h}}_{N_R} \end{bmatrix} \tag{4}$$

where $\bar{\mathbf{A}}_k = \begin{bmatrix} (\mathbf{A}_k)_I & -(\mathbf{A}_k)_Q \\ (\mathbf{A}_k)_Q & (\mathbf{A}_k)_I \end{bmatrix}_{2L \times 2N_T}$, $k = 1, 2, ..., K$, $\bar{\mathbf{h}}_j = [\ (\mathbf{h}_j)_I^T \quad (\mathbf{h}_j)_Q^T\ ]^T$, $j = 1, 2, ..., N_R$, and all the entries of $\mathbf{n}'$ are i.i.d. real Gaussian variable with distribution $\mathcal{N}(0, 1/2)$. Then, it can be got from (4) that $(\mathbf{H}')^T\mathbf{H}'$ is a $K \times K$ real matrix, whose entry at the $k1$-th row and $k2$-th column should be

$$\left[(\mathbf{H}')^T\mathbf{H}'\right]_{k1,k2} = \sum\nolimits_{j=1}^{N_R} (\bar{\mathbf{h}}_j)^T (\bar{\mathbf{A}}_{k1})^T \bar{\mathbf{A}}_{k2} \bar{\mathbf{h}}_j \tag{5}$$

where $k1, k2 = 1, 2, ..., K$. According to the properties of OSTBCs, the dispersion matrices of an OSTBC are unitary and at the same time satisfy the condition (mentioned in [16]) as $(\mathbf{A}_{k1})^H\mathbf{A}_{k2} + (\mathbf{A}_{k2})^H\mathbf{A}_{k1} = 0$ when $1 \leq k1 \neq k2 \leq K$. Therefore, it is not hard to obtain the similar result for the real form as

$$(\bar{\mathbf{A}}_{k1})^T\bar{\mathbf{A}}_{k2} + (\bar{\mathbf{A}}_{k2})^T\bar{\mathbf{A}}_{k1} = 0 \tag{6}$$

where $1 \leq k1 \neq k2 \leq K$. Then, combining (6) and the Theorem 1 in [17], we obtain that $\sum_{j=1}^{N_R}(\bar{\mathbf{h}}_j)^T(\bar{\mathbf{A}}_{k1})^T\bar{\mathbf{A}}_{k2}\bar{\mathbf{h}}_j = 0$ when $k1 \neq k2$. Thus, $(\mathbf{H}')^T\mathbf{H}'$ is a diagonal matrix. Since all the dispersion matrices are unitary, then their real form $\bar{\mathbf{A}}_{k1}$ and $\bar{\mathbf{A}}_{k2}$ are also unitary. Thereby, when $k1 = k2$, the diagonal entries $\sum_{j=1}^{N_R}(\bar{\mathbf{h}}_j)^T(\bar{\mathbf{A}}_{k1})^T\bar{\mathbf{A}}_{k2}\bar{\mathbf{h}}_j = \|\mathbf{H}\|_F^2$. So, we define a $K \times K$ real diagonal matrix $\mathbf{D} = diag\left([\|\mathbf{H}\|_F, \|\mathbf{H}\|_F, ..., \|\mathbf{H}\|_F]\right)$ and let $(\mathbf{H}')^T\mathbf{H}' = \mathbf{DD}$. Then, an equivalent real channel model of OSTBC can be obtained by multiplying both sides of equation (3) by a matched filter $\mathbf{D}^{-1}\mathbf{H}'^T$, as

$$\mathbf{y}_{eq} = \sqrt{\frac{\rho}{N_T}}\mathbf{D}\mathbf{x}_{eq} + \mathbf{n}_{eq} \tag{7}$$

where $\mathbf{y}_{eq} = \mathbf{D}^{-1}\mathbf{H}'^T\mathbf{r}'$ is a $K \times 1$ equivalent received vector obtained after match filtering; $\mathbf{n}_{eq} = \mathbf{D}^{-1}\mathbf{H}'^T\mathbf{n}'$ is a $K \times 1$ equivalent noise vector. Since all the entries in $\mathbf{n}'$ are i.i.d. and satisfy distribution $\mathcal{N}(0, 1/2)$, then its covariance matrix $\mathcal{E}(\mathbf{n}'\mathbf{n}'^T) = (1/2)\cdot\mathbf{I}_{2LN_R \times 2LN_R}$. It is not hard to prove that the covariance matrix of $\mathbf{n}_{eq}$ is $\mathcal{E}(\mathbf{n}_{eq}\mathbf{n}_{eq}{}^T) = \mathbf{D}^{-1}\mathbf{H}'^T\mathcal{E}(\mathbf{n}'\mathbf{n}'^T)\mathbf{H}'\mathbf{D}^{-T} = (1/2)\cdot\mathbf{I}_{K \times K}$. That means that the K entries in $\mathbf{n}_{eq}$ are also i.i.d. variable with distribution $\mathcal{N}(0, 1/2)$. Let $\mathbf{y}_{eq} = [y_1 \;\; y_2 \;\; ... \;\; y_K]^T$ and $\mathbf{n}_{eq} = [n_1 \;\; n_2 \;\; ... \;\; n_K]^T$, the expression (7) can be rewritten as

$$y_k = \sqrt{\frac{\rho}{N_T}}\|\mathbf{H}\|_F x_k + n_k \tag{8}$$

where $k = 1, 2, ..., K$.

We find from (8) that the MIMO channel is converted into K parallel single-input-single-output (SISO) channels and all these signals $x_1, x_2, ..., x_K$ in $\mathbf{C}$ are completely decoupled; moreover, the K signals have the same equivalent SISO channel $\|\mathbf{H}\|_F$. The derived equivalent decoupled model will play an important role in constructing the LJ-OSTBC and proving the diversity gain.

III. Code Construction

Suppose that $\mathbf{C}^{(t)} = \sum_{k=1}^{K}\mathbf{A}_k^{(t)}x_k^{(t)}$, $t = 1, 2, ..., M$, are the M codewords of OSTBC transmitted along M time blocks, respectively. Let $x_k^{(t)}$ and $\mathbf{A}_k^{(t)}$ $(k = 1, 2, ..., K)$ be the K real signals and dispersion matrices, respectively, in the t-th codeword $\mathbf{C}^{(t)}$. The corresponding received matrices are

$$\mathbf{R}^{(t)} = \sqrt{\frac{\rho}{N_T}}\mathbf{C}^{(t)}\mathbf{H}^{(t)} + \mathbf{N}^{(t)}, \quad t = 1, 2, ..., M \tag{9}$$

where $\mathbf{H}^{(t)}$ and $\mathbf{N}^{(t)}$ denote the channel matrix and noise matrix, respectively, at the t-th block of codeword transmission. According to the assumption of block fading, these channel matrices $\mathbf{H}^{(t)}$ keep unchanged within one block period and vary independently to each other at different blocks $t = 1, 2, ..., M$. From the derivation in Section II, we will have the following equivalent decoupled model, as

$$y_k^{(t)} = \sqrt{\frac{\rho}{N_T}}\|\mathbf{H}^{(t)}\|_F x_k^{(t)} + n_k^{(t)} \tag{10}$$

where $k=1,2,...,K$, $t=1,2,...,M$; $x_k^{(t)}$ denotes the k-th transmitted real signal in $\mathbf{C}^{(t)}$; $y_k^{(t)}$ is the corresponding equivalent receive signal; $n_k^{(t)}$ denotes the equivalent noise satisfying distribution $\mathcal{N}(0,1/2)$. The expression (10) mean that all the real signals in $\mathbf{C}^{(t)}$ will be carried by the equivalent SISO fading $\|\mathbf{H}^{(t)}\|_F$ under an i.i.d. real Gaussian noise. In sequence, we will consider the design of the KM real signals $x_k^{(t)}$, $k=1,2,...,K$, $t=1,2,...,M$.

Let Q_M be a M dimensional real lattice constellation [13], [15], and $\mathbf{x}\in Q_M$. The lattice point $\mathbf{x}$ is often a rotated version of common real signal vector, as

$$\mathbf{x}=\mathbf{G}_M\mathbf{s} \tag{11}$$

where $\mathbf{s}$ is $M\times 1$ real signal vector, whose components are taken from common PAM constellations; $\mathbf{G}_M$ is a $M\times M$ unitary rotation matrix. Obviously, the minimum symbol-wise Hamming distance between any two distinct signal vectors $\mathbf{s}\neq\mathbf{s}'$ is just one. But the rotation process spreads PAM points in $\mathbf{s}$ over all elements in $\mathbf{x}$, so that any two distinct lattices in Q_M have all their corresponding elements be different, i.e., the symbol-wise Hamming distance between them becomes M, which will perform better in aspect of anti-fading. More explanations about multiple dimensional lattice constellations are presented in Appendix A.

Generally, the M-dimensional signals taken from such Q_M have the ability to exploit the diversity gain from multiple independent fadings. At the same time, according to the derivation in (10), there are M equivalent SISO fadings $\|\mathbf{H}^{(t)}\|_F$, $t=1,2,...,M$ which fades independently. The idea of LJ-OSTBC is inspired by combining the two properties of lattice constellation and OSTBC. The key design is to assign the M dimensions of Q_M into M different codewords so that each dimension of Q_M can be transmitted via a different equivalent SISO fading. Thus, we choose one real signal in each codeword of $\mathbf{C}^{(1)}\sim\mathbf{C}^{(M)}$ to compose one M dimensional real vector $[x_k^{(1)},\ x_k^{(2)},\ ...,\ x_k^{(M)}]^T$, $k=1,2,...,K$. Naturally, K vectors are obtained as each codeword has K real signals. Let all these vectors be taken from Q_M, which is defined as

$$\mathbf{x}_k\triangleq[x_k^{(1)},\ x_k^{(2)},\ ...,\ x_k^{(M)}]^T\in Q_M,\quad k=1,2,...,K \tag{12}$$

The signal design of LJ-OSTBC is described more clearly in the Fig. 1. These codewords $\mathbf{C}^{(1)}\sim\mathbf{C}^{(M)}$, expressed as the linear form of dispersion matrices, are arranged at M different rows. These real signals which correspond to the same index k ($k=1,2,...,K$) compose a $M\times 1$ column vector. All the K column vectors are the lattices from Q_M. Some examples of LJ-OSTBC will be given in Appendix B.

When using a LJ-OSTBC with a certain constellation, we often mention in the remaining contents that "the LJ-OSTBC with Q_M rotated from a $\sqrt{W}$-PAM", where W is a given positive integer. That actually means that each complex signals in the code is taken from the W-QAM constellation. If the code rate is given by R, the information efficiency η of the proposed LJ-OSTBC should be $\eta=R\log_2 W$ bits per channel use (bpcu).

Substituting (12) to (10), we can obtain the equivalent model of LJ-OSTBC in terms of lattice vectors, as

$$\mathbf{y}_k=\sqrt{\frac{\rho}{N_T}}diag\left(\left[\|\mathbf{H}^{(1)}\|_F,\|\mathbf{H}^{(2)}\|_F,...,\|\mathbf{H}^{(M)}\|_F\right]\right)\mathbf{x}_k+\mathbf{n}_k \tag{13}$$

where $\mathbf{y}_k\triangleq[y_k^{(1)},\ \ y_k^{(2)},\ \ ...,\ \ y_k^{(M)}]^T$, $\mathbf{n}_k\triangleq[n_k^{(1)},\ \ n_k^{(2)},\ \ ...,\ \ n_k^{(M)}]^T$, and $k\in\{1,2,...,K\}$. The expression (13) also shows that the entries at different dimensions of lattice $\mathbf{x}_k$ do be equivalently transmitted by different

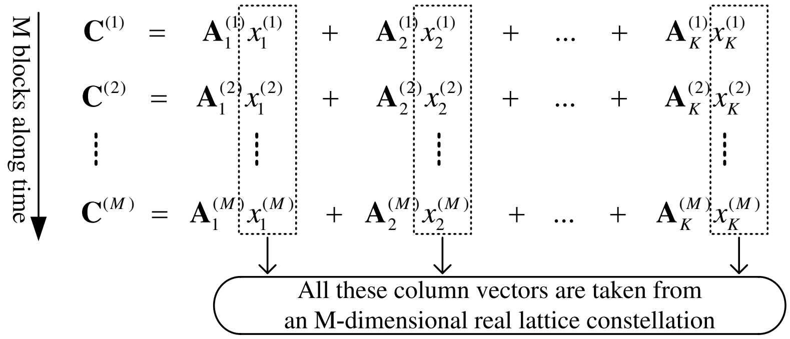

Fig. 1. Signal design for LJ-OSTBC

"fadings" $\|\mathbf{H}^{(t)}\|_F$, $t = 1, 2, ..., M$. Due to the aforementioned Hamming distance property of Q_M, the vector $\mathbf{x}_k$ will be identified in Q_M by knowing just one element at any dimension of $\mathbf{x}_k$. From intuition, the receiver is possibly able to recover the vector $\mathbf{x}_k$ as long as anyone of $\|\mathbf{H}^{(t)}\|_F$, $t = 1, 2, ..., M$, does not faded deeply. Except that all $\|\mathbf{H}^{(t)}\|_F$, $t = 1, 2, ..., M$, fall in deep fading simultaneously, $\mathbf{x}_k$ can not be recovered. But this case is very hard to arise for $\|\mathbf{H}^{(t)}\|_F$, $t = 1, 2, ..., M$ are independent on each other. Thereby, the performance of anti-fading is improved greatly without spending additional power or rate loss.

Let's consider the decoding complexity of the LJ-OSTBC. The LJ-OSTBC along M blocks include MK real signals. They are separated into K vectors $\mathbf{x}_1$, $\mathbf{x}_2$, ..., $\mathbf{x}_K$, which are uncorrelated mutually. Based on (13), the ML decoding metric of any $\mathbf{x}_k$ can be obtained as

$$\hat{\mathbf{x}}_k = \underset{\mathbf{x}_k \in Q_M}{\arg\min} \left(\sum_{t=1}^{M} \left| y_k^{(t)} - \sqrt{\frac{\rho}{N_T}} \|\mathbf{H}^{(t)}\|_F x_k^{(t)} \right|^2 \right) \tag{14}$$

where $k \in \{1, 2, ..., K\}$ and each vector $\mathbf{x}_k$ can be decoded individually. (14) means that all MK real signals in LJ-OSTBC are K-group decodable and just require M real symbols joint ML decoding, whose complexity is much lower than that of all MK signals joint ML decoding. We use the number of calculating and comparing the above ML metric to measure the decoding complexities. When the LJ-OSTBC is with Q_M rotated from $\sqrt{W}$-PAM, it is required to compute and compare the ML metric $(\sqrt{W})^M K/M$ times for each block on average.

IV. Proof of the Diversity Gain

In addition, it can be seen from (13) that each $\mathbf{x}_k$, $k \in \{1, 2, ..., K\}$ should have the same performance for they go though the same fadings and distribution of noises. Thus, we just consider anyone of them and omit the subscript k in the following performance analysis. Let $\mathbf{x} = [x^{(1)}, x^{(2)}, ..., x^{(M)}]^T$, $\mathbf{x}' = [x'^{(1)}, x'^{(2)}, ..., x'^{(M)}]^T$, and $\mathbf{x} \neq \mathbf{x}' \in Q_M$. $P(\mathbf{x} \to \mathbf{x}')$ denote the pairwise error probability (PEP), which is the probability of the received vector $\mathbf{y}$ to be closer to $\mathbf{x}'$ than to $\mathbf{x}$, assuming that the lattice point $\mathbf{x}$ is transmitted. In order to prove the diversity gain of the proposed LJ-OSTBC, we will derive the Chernoff bound of the PEP based on the ML metric in (14).

For expressing conveniently, we define that $\alpha^{(t)} \triangleq \|\mathbf{H}^{(t)}\|_F^2$, $t = 1, 2, ..., M$ and let $\mathbf{\Omega} = \left[\alpha^{(1)}, \alpha^{(2)}, ..., \alpha^{(M)}\right]$. First, supposing that $\mathbf{\Omega}$ is fixed and known, the conditional PEP is given according to (14), as

$$\begin{aligned} & P(\mathbf{x} \to \mathbf{x}'|\mathbf{\Omega}) \\ = \; & P\left(\sum_{t=1}^{M}\left|y^{(t)} - \sqrt{\tfrac{\rho\alpha^{(t)}}{N_T}}x'^{(t)}\right|^2 < \sum_{t=1}^{M}\left|y^{(t)} - \sqrt{\tfrac{\rho\alpha^{(t)}}{N_T}}x^{(t)}\right|^2\right) \\ \triangleq \; & P(X > A) \end{aligned} \tag{15}$$

where

$$X = -\sum_{t=1}^{M}\sqrt{\rho\alpha^{(t)} \big/ N_T}(x^{(t)} - x'^{(t)})n^{(t)}, \tag{16}$$

$$A = \frac{1}{2}\sum_{t=1}^{M}\left(\rho\alpha^{(t)} \big/ N_T\right)(x^{(t)} - x'^{(t)})^2. \tag{17}$$

It is not hard to see that X is a Gaussian random variable and A is a constant when the condition $\mathbf{\Omega}$ is known. Furthermore, as $n^{(t)} \sim \mathcal{CN}(0, 1/2)$, it can be derive that the mean of X is zero and the variance is $\sigma_X^2 = A$. The conditional PEP can be rewritten as $P\left(\mathbf{x} \to \mathbf{x}'\,|\mathbf{\Omega}\right) = \mathcal{Q}_{Guas}(A/\sigma_X)$, where $\mathcal{Q}_{Guas}(\cdot)$ is the Gaussian tail function $\mathcal{Q}_{Guas}(x) = (2\pi)^{-1/2}\int_x^{\infty}\exp(-a^2/2)da$, which satisfies the Chernoff bound $\mathcal{Q}_{Guas}(x) \leq \exp(-x^2/2)$. Therefore

$$P\left(\mathbf{x} \to \mathbf{x}'|\mathbf{\Omega}\right) \leq \exp\left(-\frac{A}{2}\right) = \prod_{t=1}^{M}\exp\left(-v^{(t)}\alpha^{(t)}\right) \tag{18}$$

where

$$v^{(t)} \triangleq (\rho/4N_T)\left(x^{(t)} - x'^{(t)}\right)^2 \tag{19}$$

The PEP $P\left(\mathbf{x} \to \mathbf{x}'\right)$ can be obtained by averaging over the fadings $\mathbf{\Omega} = \left[\alpha^{(1)}, \alpha^{(2)}, ..., \alpha^{(M)}\right]$, whose joint probability density function is given by $p\left(\mathbf{\Omega}\right) = p\left(\alpha^{(1)}\right)p\left(\alpha^{(2)}\right)...p\left(\alpha^{(M)}\right)$ as $\alpha^{(1)} \sim \alpha^{(M)}$ are independent to each other. Then according to (18) we can get

$$P\left(\mathbf{x} \to \mathbf{x}'\right) = \int\limits_{\mathbf{\Omega}} P\left(\mathbf{x} \to \mathbf{x}'\,|\mathbf{\Omega}\right)p(\mathbf{\Omega})d\mathbf{\Omega} \leq \prod_{t=1}^{M}P^{(t)} \tag{20}$$

where for $\forall \;\; t \in \{1, 2, ..., M\}$,

$$P^{(t)} = \mathcal{E}\left(\exp(-v^{(t)}\alpha^{(t)})\right) = \int\limits_{\alpha^{(t)}}\exp(-v^{(t)}\alpha^{(t)})p(\alpha^{(t)})d\alpha^{(t)} \tag{21}$$

In the sequel, we will analyze the probability density property of $\alpha^{(t)}$, $t = 1, 2, ..., M$. Let the channel matrix $\mathbf{H}^{(t)} = \{h_{ij}^{(t)}\}_{N_T \times N_R}$, where $h_{ij}^{(t)}$, $i = 1, 2, ..., N_T$, $j = 1, 2, ..., N_R$, $t = 1, 2, ..., M$, denotes the channel from ith transmit antenna to jth receive antenna at the t-th block. Obviously, $\alpha^{(t)} = \sum_{i=1}^{N_T}\sum_{j=1}^{N_R}|h_{ij}^{(t)}|^2$; and the probability density property of $\alpha^{(t)}$ is independent on t due to the identical statistical property for all $\mathbf{H}^{(t)}$, $t = 1, 2, ..., M$. For simplifying the expression, we define the modulus of $N_T N_R$ channels in $\mathbf{H}^{(t)}$ as $z_l = |h_{ij}^{(t)}|$, where $l = (i-1)N_R + j$, $i = 1, 2, ..., N_T$, $j = 1, 2, ..., N_R$, and t is omitted. Thus $\alpha^{(t)}$ can be rewritten as

$$\alpha^{(t)} = \sum_{l=1}^{N_T N_R} z_l^2, \quad l = 1, 2, ..., N_T N_R \tag{22}$$

Moreover, we know that all z_l, $l = 1, 2, ..., N_T N_R$ will be i.i.d and obey the standard Rayleigh distribution as $h_{ij}^{(t)}$, $i = 1, 2, ..., N_T$, $j = 1, 2, ..., N_R$ are i.i.d. and satisfy $\mathcal{CN}(0, 1)$. So, the probability density function of z_l is

$$f(z_l) = 2z_l \exp\left(-z_l^2\right), \quad l = 1, 2, ..., N_T N_R \tag{23}$$

Since z_l, $l = 1, 2, ..., N_T N_R$ are mutually independent, substituting (22) to (21), (21) can be rewritten as

$$P^{(t)} = \prod_{l=1}^{N_T N_R} \mathcal{E}\left(\exp(-v^{(t)} z_l^2)\right) \tag{24}$$

where $t = 1, 2, ..., M$. According to (23), it is not hard to derive that $\mathcal{E}\left(\exp(-v^{(t)} z_l^2)\right) = 1/(1 + v^{(t)})$, $l = 1, 2, ..., N_T N_R$. Thus, we can obtain from (24) that

$$P^{(t)} = \left(\frac{1}{1 + v^{(t)}}\right)^{N_T N_R} \tag{25}$$

Also, the equation (25) holds for any $t \in \{1, 2, ..., M\}$ due to the symmetry property. Then, substituting (19) and (25) to (20), the Chernoff bound of PEP can be given as

$$P(\mathbf{x} \to \mathbf{x}') \leq \prod_{t=1}^{M} \left(\frac{1}{1 + \frac{\rho(x^{(t)} - x'^{(t)})^2}{4N_T}}\right)^{N_T N_R} \tag{26}$$

Since $\mathbf{x} \neq \mathbf{x}' \in Q_M$ and their Hamming distance is equal to M, then any corresponding dimensions of $\mathbf{x}$ and $\mathbf{x}'$ should be unequal, i.e., $x^{(t)} - x'^{(t)} \neq 0$ for $\forall\ t \in \{1, 2, ..., M\}$. Therefore, the above "1" at the denominator in (26) can be neglected when high SNR ($\rho >> 1$). Then, the PEP can be upper-bounded by the following expression, as

$$P(\mathbf{x} \to \mathbf{x}') \leq \rho^{-MN_T N_R} \left((4N_T)^{-\frac{M}{2}} \prod_{t=1}^{M} \left(x^{(t)} - x'^{(t)}\right)\right)^{-2N_T N_R}. \tag{27}$$

The diversity gain is the power of SNR in the denominator of the PEP expression in (27). Thus, the achieved diversity gain is $MN_T N_R$ orders for the constructed LJ-OSTBCs, which is M times of the diversity gain for common STBCs. In STBCs, N_T and N_R are usually named as the orders of transmitted space diversity and received space diversity, respectively. Then M, which implies the free degrees of channel along time, is the achieved order of time diversity here. Since the proposed code obtains more diversity gain, it should have sharper slope of bit-error-rate (BER) reduction along SNR than that of common codes with only full space diversity. This point will be verified in following simulations. In addition, the coding gain is determined by the value of $\prod_{t=1}^{M} (x^{(t)} - x'^{(t)})$ from (27), which is the so-called product distance [13] from $\mathbf{x}$ to $\mathbf{x}'$. To obtain good performance, Q_M used in LJ-OSTBCs is chosen with such real lattices in [15], whose Hamming distance is always M and product distance is maximized by optimal rotation matrices.

V. Numerical Results

In this section, we give some analysis and evaluation about the performance, decoding delay and decoding complexity of the proposed LJ-OSTBCs by simulations comparison with other typical STBCs. The channels with two different fadings parameters are included here. The channel state informations are supposed being perfectly known at the receiver but unknown at the transmitter.

A. Performance Under Block-Independently Fading Channels

First, we compare the BER performance of the proposed LJ-OSTBCs with OSTBCs [1], [3], Golden code [5], and QOSTBC [4], which are some typical codes with full space diversity. The channel fadings are constant within one block and vary independently from one block to another. In Fig. 2, we show the BER performance of LJ-OSTBC for N_T=2=N_R, where three Alamouti blocks are coded jointly and Q_3 rotated from 4PAM signals are used. Accordingly, Golden code and Alamouti code use 4QAM and 16QAM, respectively. Then, all of them have the information rate 4 bpcu. Besides, we also simulate the BER of the code in [12] under 4 bpcu, which actually corresponds to the LJ-OSTBC with double Alamouti blocks jointly coded. We find that Alamouti code and Golden code, which both have 4 orders diversity, almost have parallel slopes of BER-SNR curves in high SNR area; the proposed LJ-OSTBC with M=3, which has 12 orders diversity, obtains the biggest curve slope in all these codes. As a result, the proposed LJ-OSTBC have about 4dB and 1.5dB performance gain at the BER 10^{-6} compared with Golden code and the code [12], respectively.

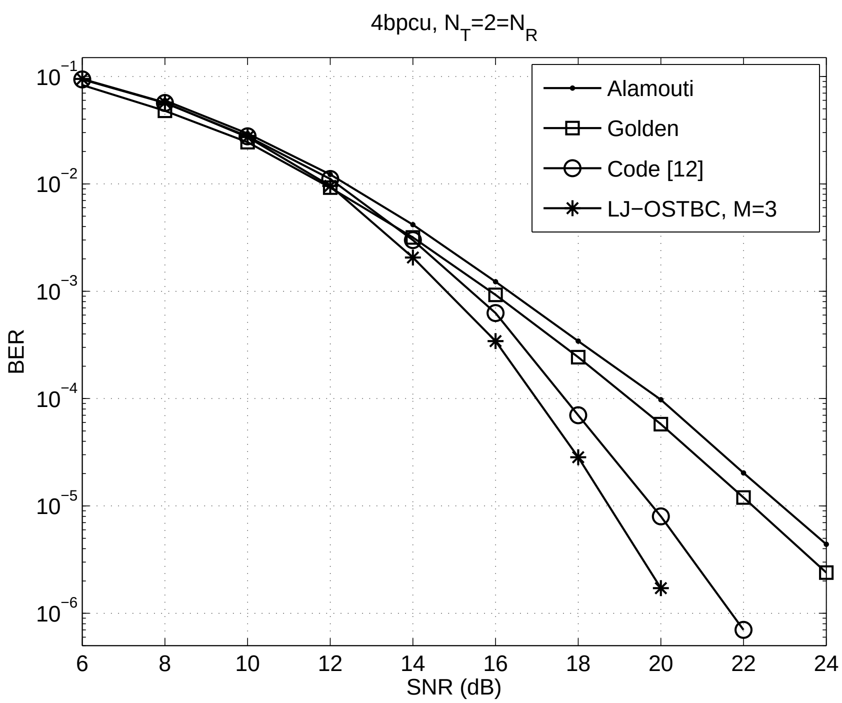

Fig. 2. Performance of the LJ-OSTBC with $M = 3$ compared to Alamouti code, Golden code and the code [12], 4bpcu, $N_T = 2$ and $N_R = 2$.

In Fig. 3, the BER comparison from OSTBC to LJ-OSTBCs with M=2, 3, 4 is given for N_T=4 and N_R=1. The OSTBC is the 4×4 code in [3] and uses 4QAM constellation; the LJ-OSTBCs with M=2, 3, 4 use the lattice constellations Q_2, Q_3, Q_4, respectively, all of which are rotated from 2PAM signals. Thus, the information rates of them are all 1.5 bpcu. Fig. 3 shows that the performance of LJ-OSTBCs improves with M increasing as the diversity gain rises; and the LJ-OSTBCs with just small M values ($M \geq 2$) can enormously outperform the common OSTBCs; the further improvement of performance will become slow when M is more than four. Thus, we usually choose $M = 2, 3, 4$ for the proposed LJ-OSTBCs so that the decoding complexity is still low.

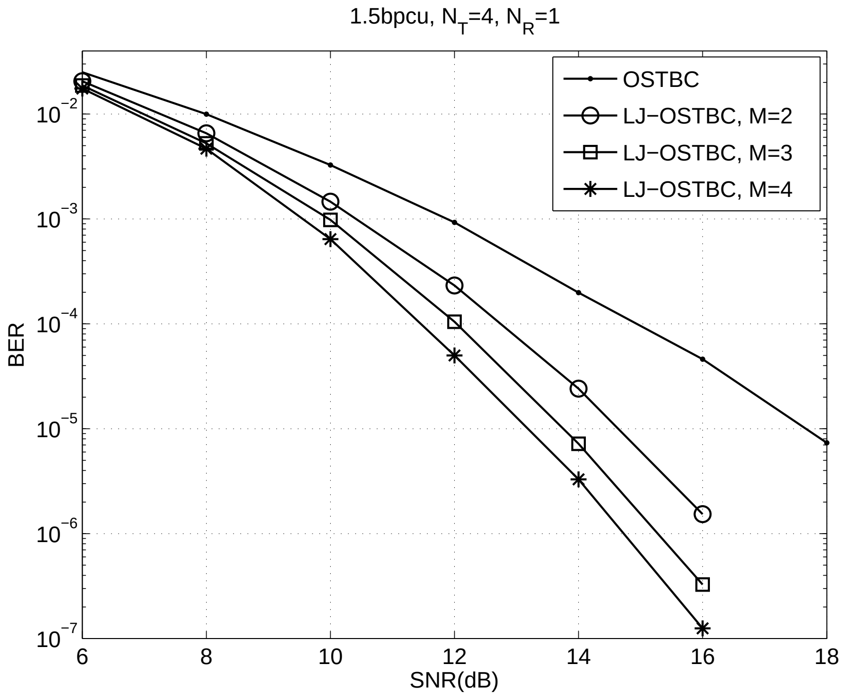

Fig. 3. Performance of the LJ-OSTBC compared to OSTBC, 1.5bpcu, $N_T = 4$ and $N_R = 1$.

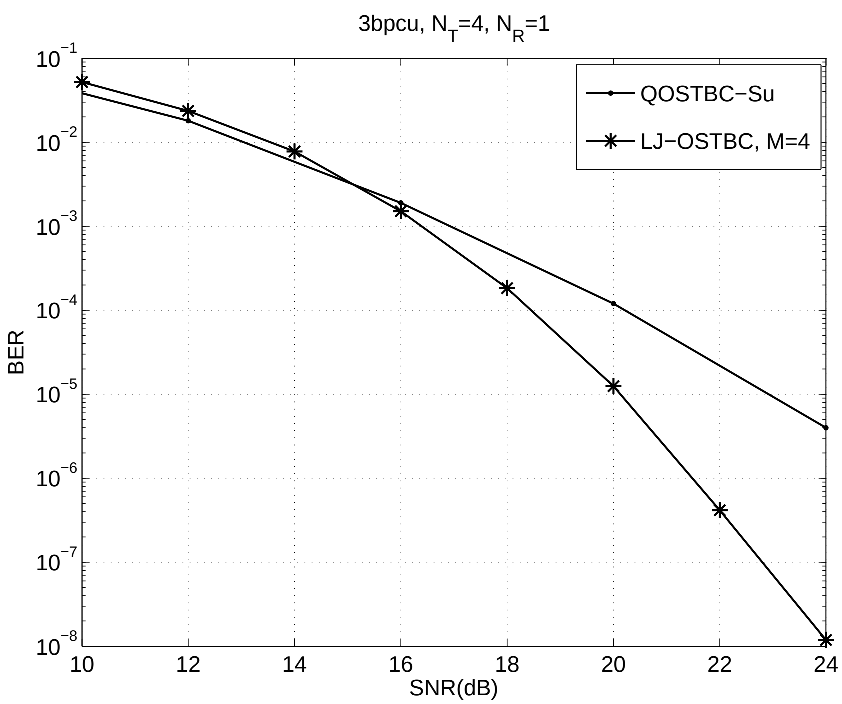

Fig. 4. Performance of the LJ-OSTBC with $M = 4$ compared to QOSTBC, 3bpcu, $N_T = 4$ and $N_R = 1$.

In Fig. 4, we compare the BER of LJ-OSTBC to the well-known 4×4 QOSTBC in [4] for N_T=4 and N_R=1 system. Let M=4, so LJ-OSTBC employs four-real-symbols joint ML decoding, whose complexity is comparable to that of QOSTBC. Besides, 8QAM constellation and Q_4 rotated from 4PAM are used for QOSTBC and LJ-OSTBC, respectively. Thus, they have the same information rate 3 bpcu. As shown in Fig. 4, though the proposed LJ-OSTBC is slightly worse than QOSTBC at low SNR, it significantly outperforms QOSTBC at high SNR regions (SNR>15dB) due to the larger slope of BER-SNR curve, where about 3dB gain is obtained at the BER 10^{-5}.

B. Performance Under Block-Correlatively Fading Channels

Though the LJ-OSTBC is designed at block-independently fading assumption, it is necessary to give an evaluation about the performance and decoding delay when the channel variation slows down. The simulation analysis is presented here when the channel exists correlation from one block to another. A typical scenario of 1.9 GHz PCS system is considered, in which the symbol rate is 6.4kBd and the speed of mobility is 112 and 250 km/h, respectively. A large Doppler spread often results in the channel time-varying with a certain correlation coefficient. We use the Jakes' model introduced in [18] to describe the relations of mobility speed, Doppler spread, coherent time and correlation coefficient. The channel fadings in different transmit-receive links are assumed to be i.i.d and the correlation coefficient is common for all links. Let $R(l)$ be the correlation coefficient from the t-th block to the $(t+l)$-th block. According to the Jakes' model, we have $R(l) = J_0\left(2\pi f_d T_B l\right)$, where $J_0(.)$ is the zeroth-order Bessel function of the first kind; f_d is the maximum Doppler spread; T_B is the period of each block. Some detailed parameters for the scenario are shown in Table I. As an example, we simulate the proposed LJ-OSTBC with $M = 3$, $N_T = 2$ and $N_R = 1$ based on lattice constellation Q_3 rotated from 2PAM, where three adjacent blocks are used to encode jointly so that the decoding delay is minimum for the proposed approach. As shown in Table I, the decoding delay is about 1/5 and 2/5 of the coherent time for the speed 112 km/h and 250 km/h, respectively.

The BER of proposed code is shown in Fig. 5 under different mobility speed. For the static case (speed=0), where the channel keeps invariant during different blocks and there is no time diversity, the proposed code has the identical performance as the original Alamouti code. For the mobile case (speed=112 km/h or 250 km/h), the channel will vary with a certain correlation from one block to another. Even if such a correlation is large (correlation coefficient is 0.9629 and 0.8217, respectively, for the above two speeds), the proposed code can still obtain significant improvement of performance. When BER=10^{-4}, compared with the static case, the proposed code has at least 3dB gain for speed 112km/h and 5dB gain for speed 250km/h. In summary, the proposed code is suitable for mobile wireless communications; the performance improves obviously by using just 2$\sim$3 adjacent blocks to jointly code, so that the decoding delay is often acceptable and is much less than the coherent time.

C. Comparisons of the Complexity of Decoding

Given by an information efficiency η, we compare the decoding complexity of the proposed LJ-OSTBC and other codes in Table II and Table III, which correspond to the cases $N_T = 2$ and $N_T = 4$, respectively. Using η and considering code rate R, the modulation orders W can be obtained by using the equation $\eta = R\log_2 W$, which is presented in Section III. The number of symbols needing jointly decoding is known for those codes. So, the equations of decoding complexity can be derived, which are related with η. Moreover, as several particular examples, the decoding complexity comparisons of those codes for $\eta = 2$ and $\eta = 4$ with $N_T = 2$ are shown in Table II, and the case $\eta = 3$ with $N_T = 4$ is shown in Table III. When $N_T = 2$, the decoding complexity of LJ-OSTBC with $M = 2, 3, 4$ are a litter higher than Alamouti code, but are lower than that of Golden code. When $N_T = 4$, the decoding complexity of LJ-OSTBC with $M = 2, 3, 4$ is basically comparable with that of QSTBC-Su [4].

VI. Conclusions

In this paper, we propose a construction method of joint OSTBC based on M dimensional lattice constellations and prove that the achieved diversity gain of the proposed code is M times of that in traditional STBCs. It is generally thought that a common STBC can obtain at most full space diversity. But the proposed code shows that the diversity gain of STBCs can further increase by exploiting time diversity simultaneously, which is a new attempt in space-time coding. The remarkable improvement of performance for proposed code is verified by numerical results by comparing with other typical STBCs. In addition, it is noteworthy that just small M value can improve the coding performance significantly, so that the relevant decoding complexity is still low and decoding

TABLE I

Simulation parameters of the mobile scenario

Carried frequency	1.9 GHZ	
Symbol rate	6.4 kBd	
Symbol period	$T_s = 1/6400 \approx 1.56 \times 10^{-4}$ second	
Block period	$T_B = 2T_s \approx 3.12 \times 10^{-4}$ second	
Speed of mobility	112km/h	250km/h
Doppler spread	f_d=197 Hz	f_d=440 Hz
Coherent time	$T_c \approx 1/f_d = 5.1 \times 10^{-3}$ second	$T_c \approx 1/f_d = 2.3 \times 10^{-3}$ second
Correlation coefficient for adjacent blocks	R(1)=0.9629	R(1)=0.8217
Decoding delay of the proposed code	$3T_B \approx 9.36 \times 10^{-4}$ second (three blocks length)	

TABLE II

Comparisons of decoding complexity given the information efficiency η when $N_T = 2$

	Alamouti code	Golden code	LJ-OSTBC $M = 2$	LJ-OSTBC $M = 3$	LJ-OSTBC $M = 4$
Modulation orders	2^{η}	$2^{\frac{\eta}{2}}$	2^{η}	2^{η}	2^{η}
Number of symbols for joint ML decoding	1 complex symbol	4 complex symbols	2 real symbols	3 real symbols	4 real symbols
Decoding complexity (the number of calculating ML metric at each block)	$2\left(2^{\eta}\right)$	$\left(2^{\frac{\eta}{2}}\right)^4$	$2\left(\sqrt{2^{\eta}}\right)^2$	$\frac{4}{3}\left(\sqrt{2^{\eta}}\right)^3$	$\left(\sqrt{2^{\eta}}\right)^4$
Decoding complexity, η=2 bpcu	8	16	8	32/3	16
Decoding complexity, η=4 bpcu	32	256	32	256/3	256

delay is usually feasible. In future work, a symbol-by-symbol time-varying fading channel, which fades with more degrees of freedom along time than the block fading case, would be considered for analogous space-time coding to make use of such time-varying property and obtain both space diversity and more time diversity.

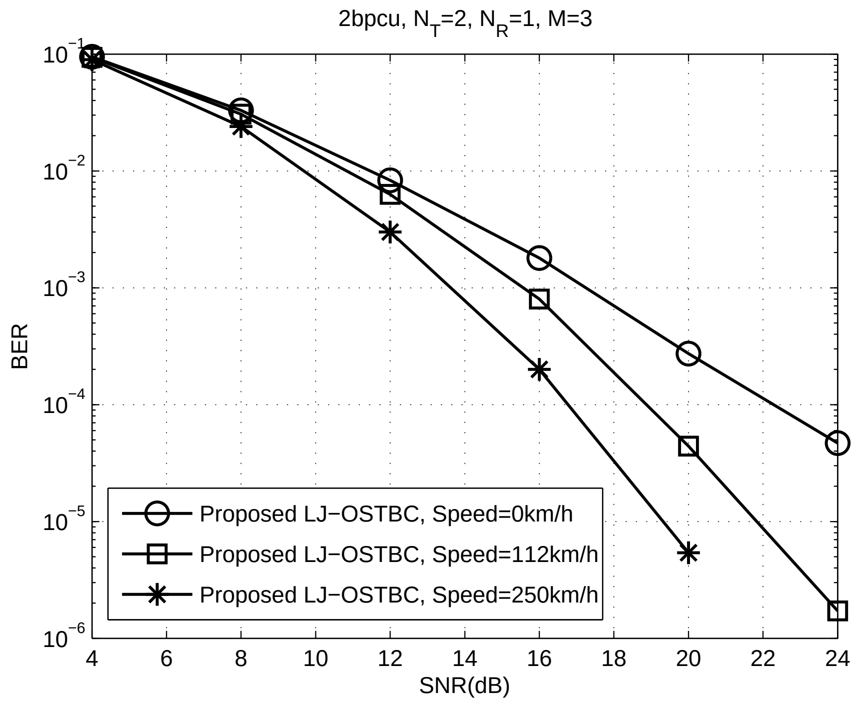

Fig. 5. Performance of the LJ-OSTBC with $M = 3$ under different mobility speeds, 2bpcu, $N_T = 2$, $N_R = 1$.

APPENDIX A
EXPLANATIONS OF MULTI-DIMENSIONAL LATTICE CONSTELLATIONS

Initially, [13] and [14] propose the concept of multi-dimensional lattice which can perform well in SISO fading channels. Later, a class of space-time block codes based on lattices are presented in [19] and [20] in MIMO channels,

TABLE III
COMPARISONS OF DECODING COMPLEXITY GIVEN THE INFORMATION EFFICIENCY η WHEN $N_T = 4$

	OSTBC	QOSTBC-Su [4]	LJ-OSTBC $M = 2$	LJ-OSTBC $M = 3$	LJ-OSTBC $M = 4$
Modulation orders	$2^{\frac{4\eta}{3}}$	2^{η}	$2^{\frac{4\eta}{3}}$	$2^{\frac{4\eta}{3}}$	$2^{\frac{4\eta}{3}}$
Number of symbols for joint ML decoding	1 complex symbol	2 complex symbols	2 real symbols	3 real symbols	4 real symbols
Decoding complexity (the number of calculating ML metric at each block)	$3 \times 2^{\frac{4\eta}{3}}$	$2(2^{\eta})^2$	$3\left(2^{\frac{2\eta}{3}}\right)^2$	$2\left(2^{\frac{2\eta}{3}}\right)^3$	$\frac{3}{2}\left(2^{\frac{2\eta}{3}}\right)^4$
Decoding complexity, η=3 bpcu	48	128	48	128	3 $\times$ 128

where the lattices can exploit just the space diversity and they still belong to common space-time codes.

Supposing $\mathbf{s} \neq \mathbf{s}'$ in (11), the lattices are $\mathbf{x} = \mathbf{G}_M\mathbf{s}$ and $\mathbf{x}' = \mathbf{G}_M\mathbf{s}'$. The rotation matrices $\mathbf{G}_M$ makes lattices satisfy the properties: 1) let $\Delta\mathbf{x} = \mathbf{x}-\mathbf{x}' \triangleq [\Delta x^{(1)}, \Delta x^{(2)}, ..., \Delta x^{(M)}]^T$, then $\Delta x^{(t)} \neq 0$ holds for $\forall\ t = 1, 2, ..., M$, so that the symbol-wise Hamming distance for any two distinct lattices is M; 2) the minimum product distance $\min\limits_{\mathbf{x}\neq\mathbf{x}'} |\prod_{t=1}^{M} \Delta x^{(t)}|$ is as large as possible. These properties make lattices perform well for anti-fading.

We give some rotation matrices $\mathbf{G}_M$ ($M = 2, 3, 4$), which are from [15] and used in this paper, as: $\mathbf{G}_2 = [\ 0.8507\ \ -0.5257;\ \ 0.5257\ \ 0.8507\ ]$, $\mathbf{G}_3 = [\ -0.3280\ \ -0.7370\ \ -0.5910;\ \ -0.5910\ \ -0.3280\ \ 0.7370;\ \ -0.7370\ \ 0.5910\ -0.3280\ ]$, and $\mathbf{G}_4 = [\ -0.3664\ -0.2264\ -0.4745\ -0.7677;\ -0.7677\ -0.4745\ \ 0.2264\ \ 0.3664;\ 0.4231\ \ -0.6846\ \ -0.5050\ \ 0.3121;\ \ 0.3121\ \ -0.5050\ \ 0.6846\ \ -0.4231\ ]$. The original vector $\mathbf{s}$ in (11) is the common $M \times 1$ real signal vector, whose components are from the real or imaginary coordinates of general QAM constellations. For instance, when complex signals are taken from W-QAM constellation, each real signal in $\mathbf{s}$ is equivalently from $\sqrt{W}$-PAM constellation. Therefore, in the simulations of this paper, it is often mentioned that "a proposed LJ-OSTBC with a certain Q_M rotated from $\sqrt{W}$-PAM".

APPENDIX B

EXAMPLES OF LJ-OSTBCS

Next, some examples of LJ-OSTBC are given. When $N_T = 2$ and $M = 3$, three Alamouti codewords [1] are coded jointly, and the corresponding LJ-OSTBC is given by (28), where $[x_k^{(1)}\ x_k^{(2)}\ x_k^{(3)}]^T \in Q_3$, $k = 1, 2, 3, 4$. When $N_T = 4$ and $M = 2$, two OSTBCs [3] are coded jointly, and the LJ-OSTBC is shown in (29), where $[x_k^{(1)}\ x_k^{(2)}]^T \in Q_2$, $k = 1, 2, ..., 6$.

$$\mathbf{C}^{(1)} = \begin{bmatrix} x_1^{(1)} + jx_2^{(1)} & x_3^{(1)} + jx_4^{(1)} \\ -x_3^{(1)} + jx_4^{(1)} & x_1^{(1)} - jx_2^{(1)} \end{bmatrix} \mathbf{C}^{(2)} = \begin{bmatrix} x_1^{(2)} + jx_2^{(2)} & x_3^{(2)} + jx_4^{(2)} \\ -x_3^{(2)} + jx_4^{(2)} & x_1^{(2)} - jx_2^{(2)} \end{bmatrix}$$
$$\mathbf{C}^{(3)} = \begin{bmatrix} x_1^{(3)} + jx_2^{(3)} & x_3^{(3)} + jx_4^{(3)} \\ -x_3^{(3)} + jx_4^{(3)} & x_1^{(3)} - jx_2^{(3)} \end{bmatrix} \tag{28}$$

$$\mathbf{C}^{(1)} = \begin{bmatrix} x_1^{(1)} + jx_2^{(1)} & x_3^{(1)} + jx_4^{(1)} & x_5^{(1)} + jx_6^{(1)} & 0 \\ -x_3^{(1)} + jx_4^{(1)} & x_1^{(1)} - jx_2^{(1)} & 0 & x_5^{(1)} + jx_6^{(1)} \\ -x_5^{(1)} + jx_6^{(1)} & 0 & x_1^{(1)} - jx_2^{(1)} & -x_3^{(1)} - jx_4^{(1)} \\ 0 & -x_4^{(1)} + jx_6^{(1)} & x_3^{(1)} - jx_4^{(1)} & x_1^{(1)} + jx_2^{(1)} \end{bmatrix}$$
$$\mathbf{C}^{(2)} = \begin{bmatrix} x_1^{(2)} + jx_2^{(2)} & x_3^{(2)} + jx_4^{(2)} & x_5^{(2)} + jx_6^{(2)} & 0 \\ -x_3^{(2)} + jx_4^{(2)} & x_1^{(2)} - jx_2^{(2)} & 0 & x_5^{(2)} + jx_6^{(2)} \\ -x_5^{(2)} + jx_6^{(2)} & 0 & x_1^{(2)} - jx_2^{(2)} & -x_3^{(2)} - jx_4^{(2)} \\ 0 & -x_5^{(2)} + jx_6^{(2)} & x_3^{(2)} - jx_4^{(2)} & x_1^{(2)} + jx_2^{(2)} \end{bmatrix} \tag{29}$$

ACKNOWLEDGMENT

The authors would like to thank the support from the National Natural Science Foundation of China (Grant Nos. 61101098).

REFERENCES

[1] Alamouti. S. M: ‘A simple transmit diversity technique for wireless communications’. IEEE J. Select. Areas Commun., vol. 16, no. 8, pp. 1451-1458, October 1998.

[2] Tarokh.V, Jafarkhani. H, and Calderbank. A. R: ‘Space-time block codes from orthogonal designs’. IEEE Trans. Inform. Theory, vol. 45, no. 5, pp. 1456-1466, July 1999.

[3] Su. W and Xia. X. G: ‘On space-time block codes from complex orthogonal designs’. Wireless Personal Commun., vol. 25, no. 1, pp. 1-26, April 2003.

[4] Su. W and Xia. X. G: ‘Signal constellations for quasi-orthogonal space-time block codes with full diversity’. IEEE Trans. Inform. Theory, vol. 50, no. 10, pp. 2331-2347, October 2004.

[5] Belfiore. J. C, Rekaya. G and Viterbo. E: ‘The Golden code: a 2x2 full-rate space-time code with nonvanishing determinants’. IEEE Trans. Inform. Theory, vol. 51, no. 4, pp. 1432-1436, April 2005.

[6] Oggier. F, Rekaya. G, Belfiore. J. C and Viterbo. E: ‘Perfect space-time block codes’. IEEE Trans. Inform. Theory, vol. 52, no. 9, pp. 3885-3902, September 2006.

[7] Srinath. K. P and Rajan. B. S: ‘Improved perfect space-time block codes’. IEEE Trans. Inform. Theory, vol. 59, no. 12, pp. 7927-7935, December 2013.

[8] Ren. T. P, Guan. Y. L, Yuen. C, Gunawan. E, and Zhang. E. Y: ‘Group decodable space-time block codes with code rate > 1’. IEEE Trans. Commun., vol. 59, no. 4, pp. 987-997, April 2011.

[9] Natarajan. L. P and Rajan. B. S: ‘Asymptotically-good, multi-group decodable space-time block codes’. IEEE Trans. Wireless Commun., vol. 12, no. 10, pp. 5035-5047, October 2013.

[10] Ren. T. P, Guan. Y. L, Yuen. C, Zhou. Y, and Zhang. E. Y: ‘Optimization of fast-decodable full-rate STBC with non-vanishing determinants’. IEEE Trans. Commun., vol. 59, no. 8, pp. 2063-2069, August 2011.

[11] Tarokh. V, Seshadri. N, and Calderbank. A. R: ‘Space-time codes for high data rate wireless communication: performance criterion and code construction’. IEEE Trans. Inform. Theory, vol. 44, no. 2, pp. 744-765, March 1998.

[12] Liu. W, Sellathurai. M, Tang. C, and Wei. J: ‘Achieving space and time diversity by using lattice constellation based joint Alamouti coding’. IEEE Commun. Letters, vol. 14, no. 1, pp. 33-35, January 2010.

[13] Boutros. J and Viterbo. E: ‘Signal space diversity: a power- and bandwidth-efficient diversity technique for the Rayleigh fading channel’. IEEE Trans. Inform. Theory, vol. 44, no. 4, pp. 1453-1467, July 1998.

[14] Boutros. J, Viterbo. E, Rastello. C and Belfiore. J. C: ‘Good Lattice Constellation for Both Rayleigh Fading and Guassian Channels’. IEEE Trans. Inform. Theory, vol. 42, no. 2, pp. 502-518, Mar. 1996.

[15] Viterbo. E: ‘Table of best known full diversity algebraic rotations’. Avalaible at: *http://www1.tlc.polito.it/ viterbo/rotations/rotations.html*

[16] Khan. M. Z. A and Rajan. B. S: ‘Single-Symbol Maximum-Likelihood Decodable Linear STBCs’. IEEE Trans. Inform. Theory, vol. 52, pp. 2062-2091, May 2006.

[17] Yuen. C, Guan. Y. L, and Tjhung. T. T: ‘Quasi-Orthogonal STBC with Minimum Decoding Complexity’. IEEE Trans. Wireless Commun., vol. 4, no. 5, pp. 2089-2094, Sep. 2005.

[18] Jakes. W. C, ‘Microwave Mobile Communication’. New York: Wiley, 1974.

[19] Damen. M. O, Karim. A. M and Belfiore. J. C: ‘Diagonal Algebraic Space-Time Block Codes’. IEEE Trans. Inform. Theory, vol. 48, no. 3, pp. 628-636, Mar. 2002.

[20] Liao. H, Wang. H, and Xia. X. G: ‘Some Designs and Normalized Diversity Product Upper Bounds for Lattice-Based Diagonal and Full-Rate Space-Time Block Codes’. IEEE Trans. Inform. Theory, vol. 55, no. 2, pp. 569-583, Feb. 2009.